PCCP

PAPER

View Article Online
View Journal | View Issue

Cite this: *Phys. Chem. Chem. Phys.*, 2018, **20**, 29648

Energy transfer and spatial scrambling of an exciton in a conjugated dendrimer

D. Ondarse-Alvarez,[a] N. Oldani,[a] A. E. Roitberg,[b] V. Kleiman,[b] S. Tretiak[c] and S. Fernandez-Alberti *[a]

Received 17th September 2018,
Accepted 14th November 2018

DOI: 10.1039/c8cp05852k

rsc.li/pccp

Photoexcitation of multichromophoric light harvesting molecules induces a number of intramolecular electronic energy relaxation and redistribution pathways that can ultimately lead to ultrafast exciton self-trapping on a single chromophore unit. We investigate the photoinduced processes that take place on a phenylene-ethynylene dendrimer, consisting of nine equivalent linear chromophore units or branches. *meta*-Substituted links between branches break the conjugation giving rise to weak couplings between them and to localized excitations. Our nonadiabatic excited-state molecular dynamics simulations reveal that the ultrafast internal conversion process to the lowest excited state is accompanied by an inner → outer inter-branch migration of the exciton due to the entropic bias associated with energetically equivalent conjugated segments. The electronic energy redistribution among chromophore units occurs through several possible pathways in which through-bond transport and through-space exciton hopping mechanisms can be distinguished. Besides, triple bond excitations coincide with the localization of the electronic transition densities, suggesting that the intramolecular energy redistribution is a concerted electronic and vibrational energy transfer process.

I. Introduction

The goal of increasing the efficiency of photovoltaic materials for harvesting solar energy requires comprehensive knowledge and control of the multiple relaxation pathways that take place after light absorption. Photoexcitation induces a large variety of processes like internal conversion, intramolecular charge and energy redistribution, and exciton self-trapping,[1] which should be optimized toward desired function. In the particular cases of multichromophoric light harvesting molecules, different inter-chromophore energy transfer pathways appear at the same time scale. According to the relative strength of couplings between chromophore units, through-space and through-bond energy transfer mechanisms compete with each other.[2] Their efficiencies depend on the relative orientation of chromophore units within the different possible molecular configurations.[3,4]

The spatial localization of electronic excitations is very sensitive to molecular distortions.[5–9] While vibrational nuclear motions drive electronic transitions during the internal conversion process, the interplay between thermal fluctuations and electronic inter-chromophoric couplings ultimately drives transient exciton delocalization, migration and self-trapping. Transient strong nonadiabatic couplings promote delocalization increasing the efficiency of interchromophore energy transfer, while situations in which the strength of thermal fluctuations does exceed the weak electronic couplings leads to localized states (*i.e.* self-trapping). In the latter case, the excitonic wavefunction maintains its localized nature at an individual chromophore with perhaps some hops around from one unit to another. Atomistic simulations of coupled electron-vibrational dynamics can help to elucidate these scenarios, providing a detailed explanation of the underlining mechanisms that contribute to the final electronic distribution across different chromophore units.[5]

Among a wide variety of multichromophoric molecular systems, branched conjugated dendrimers represent an interesting and unique molecular family because of their exceptional light-harvesting capabilities over a broad region of the solar spectrum.[10,11] Moreover, well-controlled synthesis can yield dendrimers with well-defined architecture and high degree of order.[12–16] Due to their controllable structure and potential functionalization, dendrimers are promising for a broad range of applications such as light emitting diodes (LEDs), molecular recognition and transfer, and uses in bio-organic chemistry and nanomedicine.[17,18]

In particular, the family of dendrimers comprised by linear polyphenylene ethynylene (PPE) units has been the focus of

[a] *Departamento de Ciencia y Tecnologia, Universidad Nacional de Quilmes/CONICET, B1876BXD Bernal, Argentina. E-mail: sfalberti@gmail.com*
[b] *Department of Chemistry of Chemistry, University of Florida, Gainesville, Florida 32611, USA*
[c] *Theoretical Division, Center for Nonlinear Studies (CNLS), and Center for Integrated Nanotechnologies (CINT), Los Alamos National Laboratory, Los Alamos, NM 87545, USA*

many theoretical and experimental studies.[19–24] PPE dendrimers have interesting electronic properties at the branching points. While in the ground state the *meta* branching breaks the conjugation giving rise to localized excitations,[25–27] in the excited states the linked units become dynamically coupled, and therefore the wavefunction can be delocalized.[27–29]

Since the pioneering work by Moore and coworkers, two series of PPE dendrimers have been characterized according their threefold symmetry and Cayley tree topology.[25,30–32] One group denoted "compact", is composed of equivalent units, that is, linear PPE segments having the same lengths. Dendrimers belonged to this group, in principle, do not have an intramolecular energy gradient. Therefore, their photoexcitation leads to a spatial scrambling of the exciton among equivalent chromophore units. The other group of dendrimers called "extended", combines linear PPE units of different conjugation length. They compose an ordered structure wherein the lengths of the units decrease toward the periphery, giving rise to an energy gradient from their periphery to the core. An example of the latter kind is one of the most studied system, the perylene-terminated dendrimer called nanostar.[30,31,33]

PPE dendrimers, composed of linear polyphenylene ethynylene (PPE) units present a case with weak charge transfer character. In fact, all relevant electronic states are neutral excitons well localized on single chromophore units. Since charge transfer across meta substitutions is negligible, the absorption spectra can be analyzed as the sum of contributions from separate linear PPE units.[26] Therefore, they can be described using the Frenkel exciton Hamiltonian[34–36] with Coulombic coupling between excitations localized on the linear units.[37]

Excited-state properties of both compact and extended PPE dendrimers have been studies both experimentally and theoretically.[25,33,37,38] Here, the exciton inter-chromophore migration was monitored by a variety of time-resolved spectroscopies, such as 2D electronic[39,40] and pump–probes spectroscopies[41,42] like transient absorption and time-resolved fluorescence anisotropy.[43–52] Following these experimental advances, theoretical models such as Frenkel exciton model,[53–60] have been employed to reproduce the qualitative spectral features of dendrimers. More recently, non-adiabatic molecular dynamics simulations, involving multiple coupled excited-states, has emerged as a useful technique that helps to develop a detailed picture of photoinduced dynamics of different PPE dendrimers and their building blocks.[42,61–66] They have shown to provide an exhaustive atomistic level description of the underlying photophysical processes such as exciton formation, localization/delocalization, nonadiabatic couplings, energy transfer between chromophore units and energy funneling.

In the present article, we focus on the photoinduced processes that take place in the 2nd generation PPE compact symmetric dendrimer D10 (Fig. 1(a)), expressed by the abbreviation, D*n*, where *n* indicates the number of its composition benzene units. This dendrimer has been previously studied using several theoretical methods.[67–73] In these studies, the explicit coupled electron-vibrational dynamics has not been directly modeled. Here in, we simulate its photoexcitation and

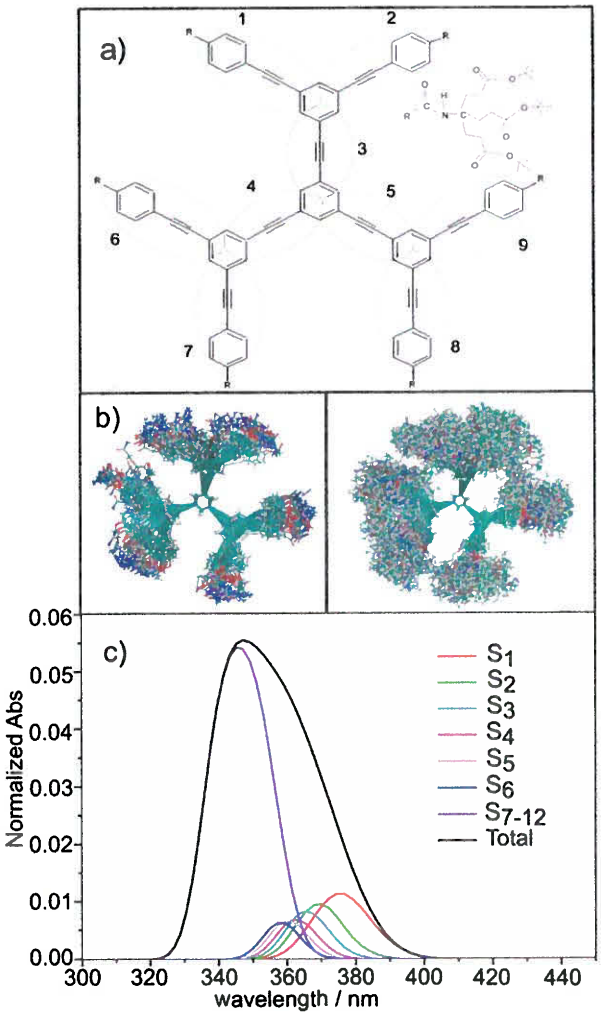

Fig. 1 (a) Chemical structure of dendrimer D10 showing the numbering pattern for the chromophore units; (b) superposition of snapshots of the D10 structure obtained from ground state molecular dynamics in THF, with and without bulky branched *t*-butyl ester ending groups demonstrating conformational diversity; (c) simulated absorption spectra with separated contributions from the different excited states.

subsequent energy relaxation and redistribution using Non-adiabatic EXcited-States Molecular Dynamics (NEXMD)[74,75] simulations. The results allow for tracking the flow of electronic transition density between chromophore units, consequently through-bond and through-space exciton transport mechanisms can be distinguished and analyzed.

II. Methods

A. The NEXMD framework

NEXMD[74,76] has been specifically developed to model photoinduced dynamics in large conjugated molecules involving multiple coupled electronically excited states. It combines surface hopping algorithm[77,78] with "on the fly" analytical calculations

of excited-state energies,[79–81] gradients,[82,83] and non-adiabatic coupling terms.[74,84–86] For this purpose, the Collective Electronic Oscillator (CEO) approach,[87–89] is used at the configuration interaction singles (CIS) level with the semiempirical AM1 Hamiltonian.[90] Our previous works show that this level of theory is accurate enough to achieve a qualitative description of the photoinduced intramolecular energy flux in PPE dendrimers.[42,61–64] Further details of the NEXMD approach, implementation, advantages and testing parameters can be found in our previous work.[74,76,91]

B. Spatial excitonic localization

NEXMD simulations allow us to follow the time evolution of the spatial excitonic localization by calculating transition density matrices $(\rho^{g\alpha})_{nm} \equiv \langle \phi_\alpha(\boldsymbol{r};\boldsymbol{R}(t))|c_m^+ c_n|\phi_g(\boldsymbol{r};\boldsymbol{R}(t))\rangle$ (denoted electronic normal modes).[92,93] Here $c_m^+(c_n)$ represents the creation (annihilation) electronic operator; and indices n and m refer to atomic orbital (AO) basis functions. In molecular system with Frenkel-type excitons such as present case, the diagonal elements $(\rho^{g\alpha})_{nn}$ are relevant to the changes in the distribution of electronic density induced by photoexcitation from the ground state g to an excited electronic α state.[94] PPE compact dendrimer D10 is fragmented into 9 individual two-ring linear polyphenylene ethynylene (PPE) chromophore units, as shown in Fig. 1(a). According to the normalization condition $\sum_{n,m} \left(\rho^{g\alpha}_{nm}(t)\right)^2 = 1$,[81] the fraction of the transition density localized on each linear PPE unit is obtained as

$$\delta_X^\alpha(t) = \left(\rho^{g\alpha}(t)\right)_X{}^2 = \sum_{n_A m_A} \left(\rho^{g\alpha}(t)\right)_{n_A m_A}{}^2 + \frac{1}{2}\sum_{n_B m_B} \left(\rho^{g\alpha}(t)\right)_{n_B m_B}{}^2 \quad (1)$$

where the index A runs over all atoms localized in the X chromophore unit ($X = 1, \ldots, 9$), and the index B runs over atoms localized in between these units. Consequently, in our case $\sum_X \delta_X^\alpha(t) \approx 1$ since *meta*-substitutions localize the excitation. In order to measure the extent of (de)localization of the excitation among the units, we define the chromophore-unit participation number,[95,96] as

$$\mathrm{PN}(t) = \left[\sum_X \left(\delta_X^\alpha(t)\right)^2\right]^{-1} \quad (2)$$

Values of $\mathrm{PN}(t) \approx 1$ indicate a complete localization of the transition density to a single chromophore unit, while values of $\mathrm{PN}(t) \approx 9$ correspond to transition densities fully delocalized across the dendritic molecule.

C. Spatial molecular scrambling

The spatial molecular scrambling is monitored using the following procedure:[97]

(1) $\mathrm{PN}(t_0)$ is evaluated at t_0.

(2) The nine chromophore units of D10 are sorted by decreasing values of $\delta_X^\alpha(t_0)$.

(3) A vector $v(t_0)$ is constructed, where the elements $v_i(t_0)$, associated to each unit, are

= 1 if $s_i < \mathrm{PN}(t_0)$

= 0 otherwise

Here s_i is the rank of the ith element according to 2.

(4) Steps 1 to 3 are repeated throughout the simulation at every time-step t, keeping the initial assignment given at t_0.

The resulting ith element of vector $v(t)$, averaged over the entire ensemble of trajectories, represents the probability of the ith chromophore unit to retain a significant contribution to $\rho^{g\alpha}(t)$. This quantifies participation of every unit in the electronic dynamics following photoexcitation, thus allowing tracking the spatial molecular scrambling of the excited state wavefunction.

D. Exciton migration dynamics

The intramolecular energy redistribution subsequent to the initial photoexcitation of D10 dendrimer is monitored by applying the transition density flux analysis,[98] originally developed by Soler *et al.*[99] to analyze the vibrational energy flow in polyatomic molecules. While the method has been presented in a previous work,[98] for the sake of completeness, we briefly outline its basic equations below.

During NEXMD simulations, at each time interval Δt, the effective change of $\delta_X^\alpha(t)$ ($\Delta\delta_X(t)$), where the superindex indicating the current state α for the NEXMD propagation has been omitted) is monitored by the flow matrix $F(t)$ with diagonal elements of zero and off-diagonal elements $f_{XY}(t)$ containing the amount of $\delta_X(t)$ transferred between units X and Y. We classify chromophore units as donors (D) if $\Delta\delta_X(t) < 0$ or acceptors (A) if $\Delta\delta_X(t) > 0$. By imposing the minimum flow criterion, that assumes that the amount of $\Delta\delta_X(t)$ is a minimum, we consider only the effective $\delta_X(t)$ flows from D to A. The total transition density exchanged among units during Δt is

$$\Delta\delta_{\mathrm{total}}(t) = \sum_{X\in \mathrm{D}} |\Delta\delta_X(t)| = \sum_{Y\in \mathrm{A}} \Delta\delta_Y(t) \quad (3)$$

And elements $f_{YX}(t)$ are calculated as

$$f_{XY}(t) = -f_{YX}(t) = \begin{cases} \dfrac{|\Delta\delta_X(t)|\Delta\delta_Y(t)}{\Delta\delta_{\mathrm{total}}(t)} & X \in \mathrm{D},\ Y \in \mathrm{A} \\ 0 & X, Y \in \mathrm{D} \text{ or } X, Y \in \mathrm{A} \end{cases} \quad (4)$$

A detailed derivation of eqn (4) can be found elsewhere.[98]

E. Computational details

Our NEXMD simulations were performed on D10 dendrimer at room (300 K) temperature. The initial conditions for these simulations have been generated from an equilibrated ground state molecular dynamics simulation of 1 dendrimer molecule solvated with 1939 explicit tetrahydrofuran (THF) molecules with periodic boundary in a box with density = 0.891 g cm^{-3}. This was carried out using the AMBER 14 software package using the GAFF (General Amber Force Field).[100,101] During simulations, a time step of 1 fs has been used and temperature

was equilibrated by employing a Langevin thermostat (with viscosity constant $\gamma = 2.0$). Electrostatic potential (ESP) derived charges for previously optimized D10 geometry were obtained from single-point BLYP/6-31G* calculations and the Merz-Kollman scheme. Restricted ESP (RESP) charges[102,103] were obtained by imposing symmetry on equivalent atom types. After minimization, the system was heated to 300 K during 100 ps, followed by 40 ns of *NPT* molecular dynamics simulation. After an equilibration of 50 ns, the NEXMD initial structures were collected every 100 ps intervals during 50 ns. These collected structures were finally relaxed during a short molecular dynamics run using the semi-empirical AM1 Hamiltonian and explicit THF molecules have been removed. That is, THF have been considering in order to generate the adequate initial conformational sampling.

Four hundred (400) individual NEXMD simulations were started from these initial configurations. The initial excited state was populated according to a Frank–Condon window given by $g_\alpha(\boldsymbol{r},\boldsymbol{R}) = f_\alpha \exp[-T^2(E_{\text{laser}} - \Omega_\alpha)^2]$ where Ω_α and E_{laser} represent the energy of the αth excited state and the energy of a laser pulse was centered at 347 nm, respectively, and f_α represents the normalized oscillator strength for the αth state. A Gaussian laser pulse, $f(t) = \exp(-t^2/2T^2)$ with $T^2 = 42.5$ fs corresponding to a FWHM (Full Width at Half Maximum) of 100 fs has been used.

Each NEXMD trajectory was propagated for 500 fs using constant-temperature at 300 K with a friction coefficient of 20.0 ps^{-1}. Excited state simulations have been performed by initially removing the bulky end-groups of D10 dendrimer. Twenty electronic states and their corresponding non-adiabatic couplings were included in the simulations. A classical time step of 0.1 fs has been used for nuclei propagation and a quantum time step of 0.025 fs has been used to propagate the electronic degrees of freedom. In order to identify and track trivial unavoided crossings, we used the Min-Cost algorithm as it has been described elsewhere.[104] In addition instantaneous decoherence approach, where the electronic wavefunction is collapsed following attempted hop (either successful or forbidden), was introduced to account for electronic decoherence.[105] More details concerning the NEXMD implementation and parameters can be found elsewhere.[76,91,106]

III. Results and discussion

We study the photoexcitation and subsequent energy relaxation and redistribution in the compact PPE dendrimer D10 (Fig. 1(a)) with a backbone containing nine equivalent 1,4-phenylethynyl chromophore units with bulky branched *t*-butyl ester ending groups. The presence of these ester groups makes the D10 dendrimer soluble in organic solvents like THF but does not affect its photophysical properties. Nevertheless, these bulky end-groups modulate the conformational diversity of D10[107] by introducing steric hindrance for the torsional motion of chromophore units. This is revealed in Fig. 1(b) that shows the superposition of snapshots obtained from the ground state molecular dynamics of D10 in THF, with and without bulky branched *t*-butyl ester ending groups demonstrating conformational diversity (compare the right and left panels of the figure). These collected structures (obtained in the presence of bulky ending groups) were used to simulate the absorption spectrum shown in Fig. 1(c). This spectrum directly reflects effect of the torsional broadening caused by thermal fluctuations. The calculated absorption maximum appears at slightly lower energies than the experimental,[25] which was already reported for other PPE dendrimers using the same level of theory.[42,61–64] This systematic deviation was shown to have minor effect on a description of PPE excited-state dynamics.

The spatial localization of different excited states that contribute to the absorption spectrum, is analyzed in Fig. 2. The distribution of values of PN(0) (see eqn (2)) for each excited state, obtained from an ensemble of the initial ground state conformations, is shown in Fig. 2(a). We observe that the lowest

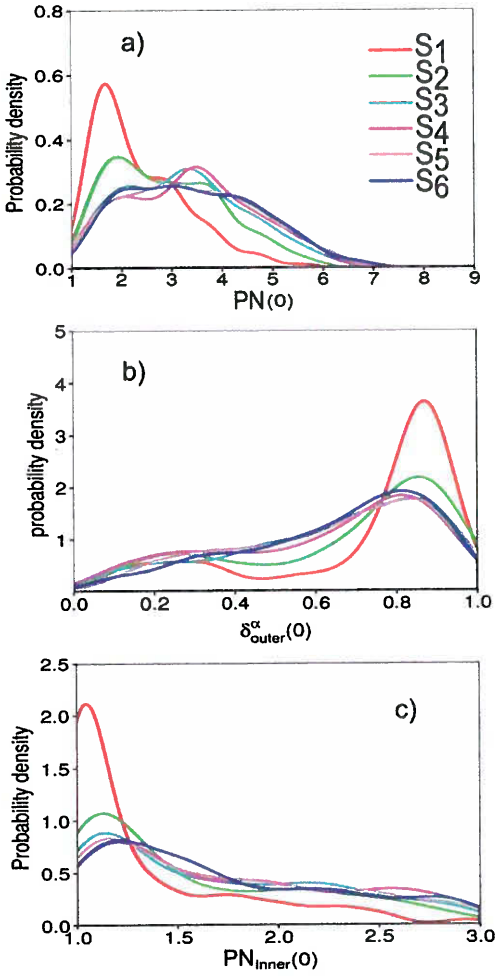

Fig. 2 Analysis of the spatial localization of the exciton on the different excited states evaluated for the ensemble of the initial ground state conformational sampling: (a) distribution of PN(0) values; (b) distribution of the transition density fraction localized on the six outer units ($\delta^{\alpha}_{\text{outer}}(0)$); (c) distribution of $PN_{\text{inner}}(0)$ values.

S_1 excited state is nearly localized on two chromophore units. The excited states become more delocalized across different equivalent units with increasing their energies. The broadness of distributions reflects the impact of conformational diversity of dendrimer D10 at room temperature. The nature of the electronic states and the extent of coupling between units significantly change with structural distortions introduced by thermal fluctuations.[64,74] A further analysis of the exciton localization can be seen in Fig. 2(b) that displays the fraction of transition density localized on the six outer units of D10, that is, $\delta^{\alpha}_{\text{outer}}(0) = \sum_{X\in\text{outer}} \delta^{\alpha}_{X}(0)$ (X = 1, 2, 6, 7, 8, and 9, following the notation given in Fig. 1(a)). It can be seen that S_1 state is mainly localized on the external units and the degree of localization on these units decreases with an increase of state energy. Nevertheless, as shown in Fig. 2(a), the distributions are quite wide. Finally, the distribution of the exciton among the inner units, *i.e.*, units 3, 4, and 5, is analysed in Fig. 2(c) that shows the distribution of values of the participation number $\text{PN}_{\text{inner}}(0)$ for each excited state, evaluated over the $\delta^{\alpha}_{X}(t)$ localized on inner units, that is,

$$\text{PN}_{\text{inner}}(t) = \left[\sum_{X\in\text{inner}} \left(\frac{\delta^{\alpha}_{X}(t)}{\sum_{Y\in\text{inner}} \delta^{\alpha}_{Y}(t)}\right)^{2}\right]^{-1} \quad (5)$$

As pointed out in Fig. 2(a and b), S_1 state is the most localized state and distributions become wider for higher energy states. That is, not only the fraction of transition density localized on inner units (Fig. 2(b)) but also the extent of exciton delocalization among these units increases with the state energy. Nevertheless, the broad distributions shown in Fig. 2(a–c) are indicative that exciton localization among the nine equivalent units of dendrimer D10 is very sensitive to molecular conformation.

The photoinduced intramolecular electronic energy relaxation and redistribution of dendrimer D10 was further studied using NEXMD simulations. The evolution in time of electronic state populations is shown in Fig. 3. The initial photoexcitation populates S_9 to S_{16} states that further experience ultrafast

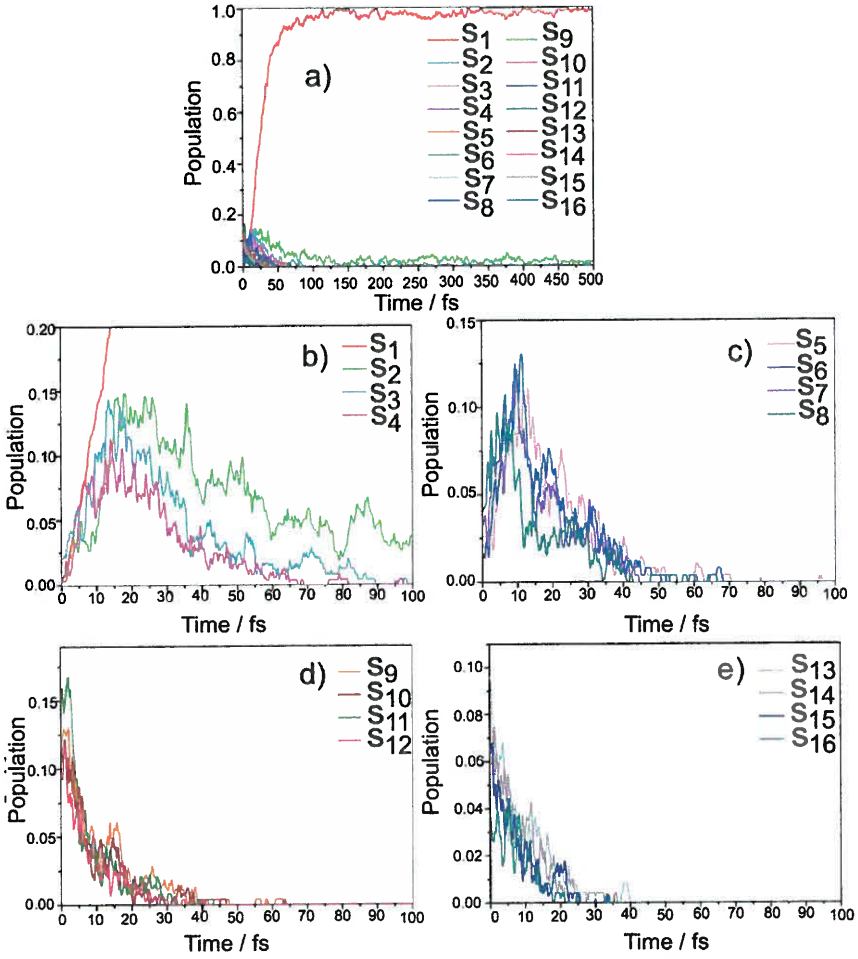

Fig. 3 Time evolution of electronic state populations for states (a) S_1–S_{16} along the entire trajectory; (b) S_1–S_4; (c) S_4–S_8; (d) S_9–S_{12}; (e) S_{13}–S_{16} during the first 100 fs after photoexcitation.

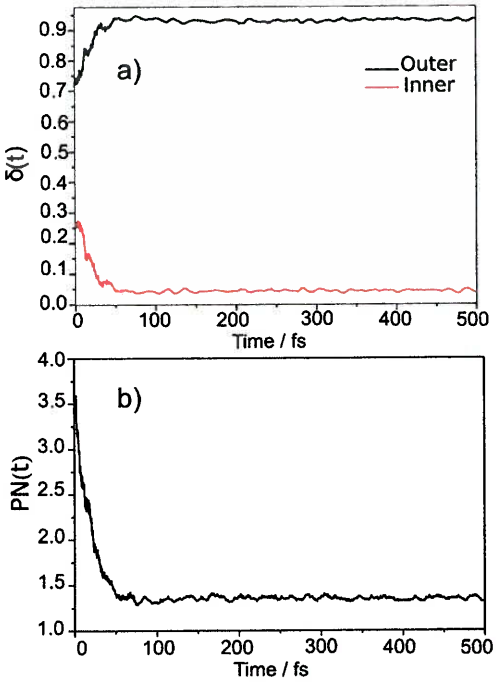

Fig. 4 (a) Time evolution of the average over all trajectories of (a) fraction of transition density localized on the six outer ($\delta_{outer}(t)$), and three inner ($\delta_{inner}(t)$) units of D10; (b) variation of participation number PN(t).

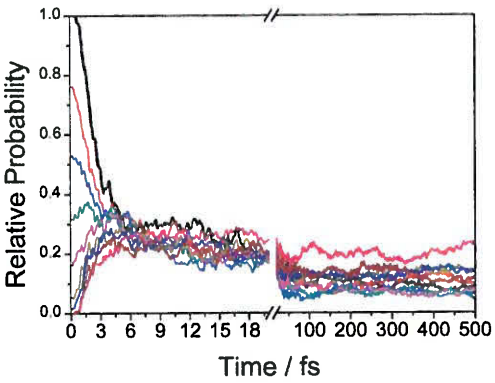

Fig. 5 Time evolution of the relative probability for each chromophore unit to retain a significant contribution to total electronic transition density during simulations. The different colors indicate the different chromophore unit ordered by decreasing contribution to the initial electronic transition density.

relaxation to intermediate S_3 to S_8 states during the first ~50 fs after photoexcitation. The S_2 state also acts as an intermediate state at longer times. Finally, the lowest S_1 state gains nearly all population within the first 100 fs of the NEXMD simulations. During this time the exciton undergoes a directional intramolecular migration from the inner units to the outer. This can be seen in Fig. 4(a) displaying the time evolution of the fraction of transition density localized on the six outer ($\delta_{outer}(t)$) and three inner ($\delta_{inner}(t)$) units of D10. This unidirectional exciton migration to the dendrimer periphery has been previously reported by Suzuki *et al.*[108] using a model Hamiltonian in which each phenyl ring is represented as a two-level system. This model accounts for an optimized dendritic structure and points to the essential role of the treelike dendrimer structure in the intramolecular exiton redistribution. Herein, we directly verify this ultrafast inner → outer exciton migration using an average of a realistic ensemble of equilibrated dendritic structures at room temperature. Concomitantly with this process, an ultrafast exciton self-trapping at periphery can be observed. Fig. 4(b) displays the time evolution of PN(t) (see eqn (2)) after photoexcitation. An initial exciton delocalized among 3–4 units, is subsequently getting self-trapped on a single unit. This is in agreement with the gradual increase of the spatial localization of states with decrease the state energy (see Fig. 2). Therefore, during the initial ~100 fs of photoexcited dynamics, our simulations reveal three concomitant processes: ultrafast internal conversion toward the lowest S_1 excited state, intramolecular inner → outer exciton migration and exciton self-trapping on a single unit at periphery.

In order to further analyse the dynamical aspects of exciton redistribution among various chromophore units, the probability of each unit to retain a significant contribution to $\rho^{g\alpha}(t)$ is tracked following the procedure described in Section IIC. Fig. 5 shows an ultrafast participation of all the units during the internal conversion process. The 3–4 units that initially hold the exciton, rapidly transfer it to the rest leading to a spatial molecular scrambling of the excited state wavefunction with the exciton equally distributed among all linear chromphores. This result suggests that the electronic energy relaxation is a collective process that encompasses all equivalent chromophore units of the branched treelike structure of the compact dendrimer. Nevertheless, taking into account the ultimate inner → outer exciton migration, we observe that the transient equal distribution of the exciton across all units is partially broken at longer times (*i.e.* after the initial ~100 fs).

The different inter-unit energy relaxation pathways that lead to the final exciton self-trapping can be identified using the transition density flux analysis described in Section IID. Fig. 6 and 7 show the time evolution of $\delta_X(t)$–$\delta_X(0)$ for each of the chromophore units. In addition to the accumulated transition density, fluxes $f_{XY}(t)$ are also displayed. In order to average results obtained in different NEXMD simulations, unit 1 is labeled as the one that ultimately localizes the exciton at the end of each simulation. Once the unit 1 has been selected for each trajectory, the other units are numbered following the pattern shown in Fig. 1(a).

Fig. 6(a) shows the accumulation of population in unit 1 received from all other units after photoexcitation. While most of its population is transfer from outer units (2, 6, 7, 8, and 9), a small contribution (particularly at earlier times of dynamics) comes from the inner units (3, 4, and 5) (see also Fig. 6(c–e)). After an initial ultrafast accumulation of transition density during the first ~100 fs, there is a slower energy transfer from all the outer units to the unit 1 being a designated acceptor.

It is important to stress that after 100 fs the molecule is already relaxed to its lowest S_1 excited state (Fig. 3) and the

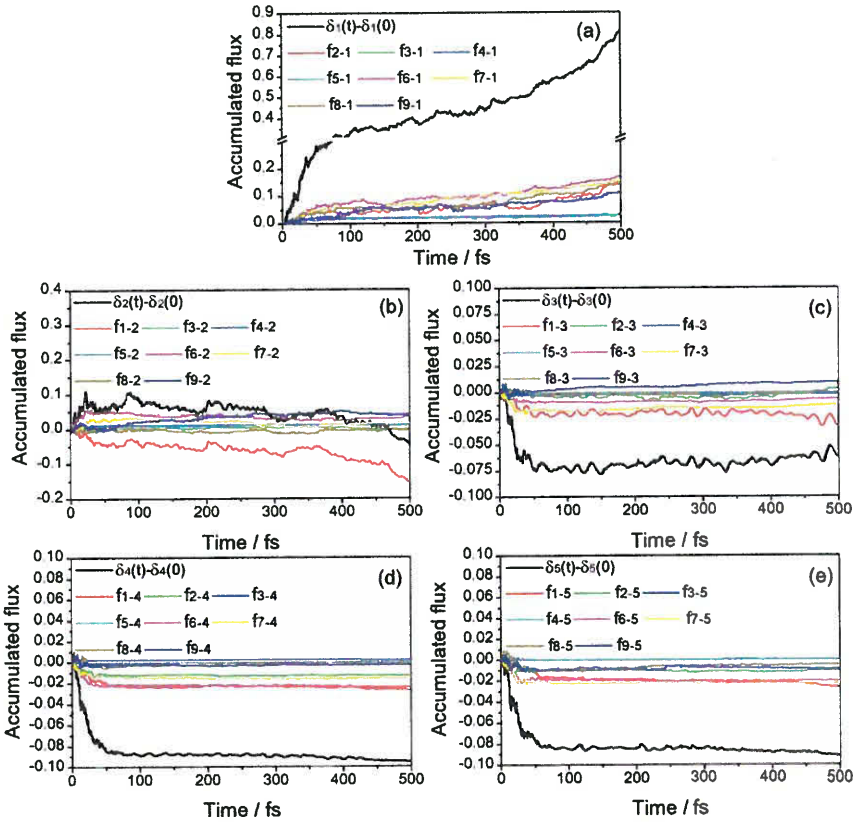

Fig. 6 Accumulated flux for units 1, 2, 3, 4, and 5 in D10 computed using the transition density flux analysis. Units are numbered according to the pattern shown in Fig. 1(a).

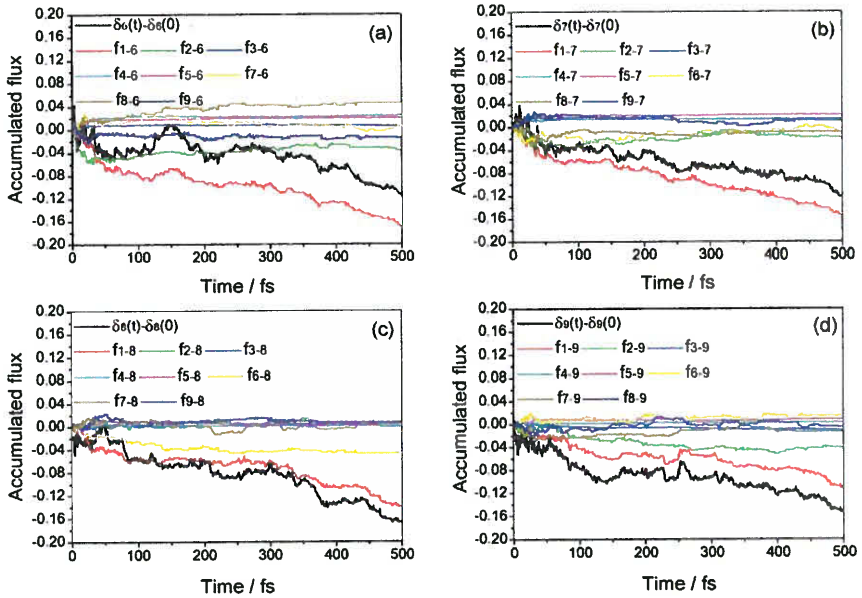

Fig. 7 The same as Fig. 6 but for units 6, 7, 8 and 9.

exciton is localized on one outer unit (Fig. 4(a and b)). Therefore, the exciton transfer to unit 1 after 100 fs is essentially a migration of the excitation across the outer units. Herein, the observed redistribution may involve several distinct pathways

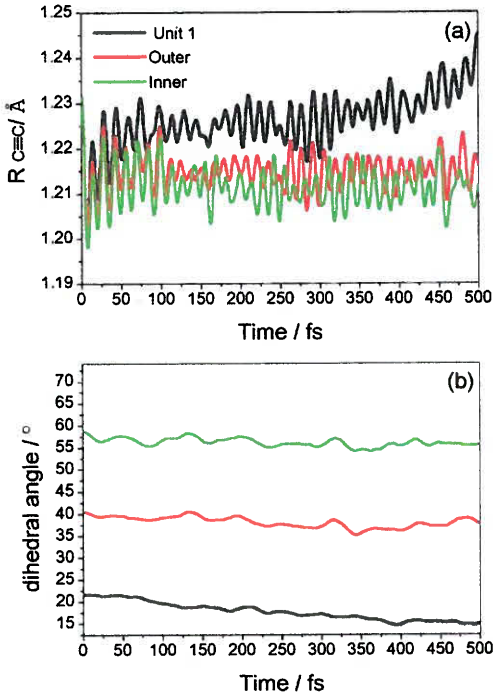

Fig. 8 Time evolution of the average over all trajectories of (a) lengths of ethynylene bonds localized on unit 1 as well as averaged over inner and outer units; (b) dihedral angles between phenyls of unit 1, and between phenyls of each individual units averaged over the ensemble of inner and outer units.

with different efficiencies. Specifically, we can distinguish between through-space (hopping) and through-bond energy transfer mechanisms. Both are expected to co-exist and compete.[63,108] The through-space path is mediated by strong interactions of outer units, which is originated from branched treelike structure. Fig. 7(a–d) indicates that the exciton itinerates by hopping on the periphery. That is, the exciton can migrate over the dendrimeric structure without passing through the core units. Additionally, Fig. 6(b) shows that minor contributions come from energy transfer pathways involving units $6,7,9 \xrightarrow{\text{through-space}} 2 \xrightarrow{\text{through-bond}} 1$. Meanwhile, inner units 3, 4, and 5 do not interchange transition density except at the beginning of dynamics. These results agree well with previous experimental and theoretical reports on compact dendrimers.[108,109] Finally, it is interesting to note that we do not observe any preferential relative orientation or distance between chromophore units that can lead to enhancement or reduction of the relative contributions of through-space and through-bond energy transfer pathways. Our NEXMD simulations have been performed at room temperature, where dendrimer D10 presents large conformational diversity (see Fig. 1(b)) with significant torsional broadening. Besides, Fig. 6 and 7 show that, within the spatial limits of the PPE compact dendrimer D10, all chromophore units show efficient through space energy transfers to unit 1, regardless the distance between them.

Previous studies of PPE dendrimer building blocks[61–63,65] have shown that intramolecular vibrational energy redistribution takes place concomitantly with the electronic energy redistribution. The nuclear motions in the direction of the stretching of ethynylene bonds (C≡C) play a critical role in this process. It has been shown that these motions represent the main contribution to the coupling between states during nonadiabatic transitions.[110] Therefore, the ethynylene bond lengths are a convenient descriptor for monitoring the intramolecular vibrational energy redistribution. Fig. 8(a) shows the evolution in time of the average over all simulations of lengths of particular ethynylene bonds localized on unit 1, inner and outer units. We can observe that after ~100 fs, an average over the outer triple bonds becomes slightly more elongated compared to the inner ones. Besides, triple bond associated with the unit 1 becomes more excited even before 100 fs, reaching progressively its larger values at the end of our simulations. That is, the electronic energy transfer is concomitant to the vibrational energy transfer through dominant C≡C stretching motions.

Finally, we explore the behaviour of dihedral angles between phenyls of the same chromophore units. Previous experimental and theoretical studies have shown planarization of *para*phenylene moieties as a general phenomenon that takes place after $\pi \rightarrow \pi^*$ electronic excitations in conjugated molecules.[9,97,111–113] Fig. 8(b) displays the time-evolution of dihedral angles between phenyls of the unit 1, and between phenyls of each individual units averaged over the ensemble of inner and outer units. The plot demonstrates that initially the inner units have much larger torsional distortion compared to that in the outer ones. The unit 1 appears as the chromophore on the periphery with the least torsions and subsequently the lowest S_1 energy. This rationalized observed trends in energy migration. Furthermore, we observe over the simulation time that dihedral angles for both inner and outer units experience only minor planarizations compared to dihedral angle of unit 1. Differences between initial and final angles, averaged over all NEXMD simulations, are 3°, 3° and 7° for inner, outer and unit 1, respectively.

IV. Conclusions

Dendrimers are multichromophoric molecular systems with well-controlled 3D structure that allow significant synthetic freedom to design and control photophysical processes that take place after light-absorption. Intramolecular migration of electronic excitations, spatial molecular scrambling and/or exciton self-trapping are consequence of geometry and topology of their highly branched treelike structure resulting in specific couplings between chromophore units and exciton transient localization/delocalization.

Herein, we have performed non-adiabatic excited state molecular dynamics simulations of the 2nd generation PPE compact dendrimer D10. Our analysis of the exciton localization/delocalization among the nine equivalent units representing elementary building blocks, reveals a significant dependence of the nature of excited states on the conformational structure of the dendrimer.

During the earliest times of dynamics after photoexcitation (~100 fs), the dendrimer experiences three concomitant

processes: ultrafast internal conversion process that relaxes its electronic energy to the lowest S1 excited state, intramolecular inner → outer exciton migration and exciton self-trapping on a single outer unit. After this ultrafast dynamics when the electronic energy is actively depositing into vibrations, the exciton itinerates among the outside of the branch until it is get trapped on the final single chromophore unit that corresponds to the final time of our simulations and equilibrium with bath degrees of freedom. Herein, the exciton redistribution may be achieved *via* several distinct pathways with different efficiencies including through-space (hopping) and through-bond energy transfer mechanisms. We observe that such exciton migration over the dendrimeric structure occurs without passing through the core.

Our simulations reveal several distinct aspects of the complex photoinduced dynamics in compact dendrimers such as electronic energy relaxation, exciton transient delocalization/localization, intramolecular migration, hopping and self-trapping. The threefold symmetry, the Cayley tree topology[25] and conformational diversity at room temperature all have significant impacts on the optical and dynamics properties of the different excitonic states. The interaction among crowded chromophore units at the molecular periphery induces a competition between through-bond and through-space energy transfer between units. Calculated ultrafast intramolecular vibrational energy redistribution activated by excited state dynamics is concomitant to the electronic energy migration. Observed differential planarization and ethynylene bond excitations of chromophore units, picture characteristic nuclear signatures of the exciton self-trapping during the photoinduced dynamics that leads to efficient fluorescence from the lowest energy electronic state in PPE dendrimers in accordance with Kasha's rule.[114] Thus, detailed information on excited state dynamics processes and photoinduced pathways delivered by atomistic simulations may provide useful reference and guideline to future and experimental and synthetic efforts in the area of molecular light harvesters.

Conflicts of interest

There are no conflicts to declare.

Acknowledgements

This work was partially supported by the National Science Foundation Grant (CHE-1802240), CONICET, UNQ, ANPCyT (PICT- PICT-2014-2662) and the U.S. Department of Energy and Los Alamos LDRD funds. Los Alamos National Laboratory is operated by Los Alamos National Security, LLC, for the National Nuclear Security Administration of the U.S. Department of Energy under contract DE-AC52-06NA25396. We acknowledge support of Center for Integrated Nanotechnology (CINT) and Center for Nonlinear Studies (CNLS) at LANL.

References

1 T. Nelson, S. Fernandez-Alberti, A. E. Roitberg and S. Tretiak, Electronic Delocalization, Vibrational Dynamics, and Energy Transfer in Organic Chromophores, *J. Phys. Chem. Lett.*, 2017, **8**, 3020–3031.
2 W. Barford, *Electronic and Optical Properties of Conjugated Polymers*, Oxford University Press, 2013.
3 M. V. Ivanov, S. H. Wadumethrige, D. Wang and R. Rathore, Through-Space or Through-Bond? the Important Role of Cofaciality in Orbital Reordering and Its Implications for Hole (De)stabilization in Polychromophoric Assemblies, *J. Phys. Chem. C*, 2017, **121**, 15639–15643.
4 N. Karakostas, A. Kaloudi-Chantzea, E. Martinou, K. Seintis, F. Pitterl, H. Oberacher, M. Fakis, J. K. Kallitsis and G. Pistolis, Energy transfer within self-assembled cyclic multichromophoric arrays based on orthogonally arranged donor–acceptor building blocks, *Faraday Discuss.*, 2015, **185**, 433–454.
5 T. Nelson, S. Fernandez-Alberti, A. E. Roitberg and S. Tretiak, Conformational disorder in energy transfer: beyond Forster theory, *Phys. Chem. Chem. Phys.*, 2013, **15**, 9245–9256.
6 J. C. Bolinger, M. C. Traub, J. Brazard, T. Adachi, P. F. Barbara and D. A. Vanden Bout, Conformation and energy transfer in single conjugated polymers, *Acc. Chem. Res.*, 2012, **45**, 1992–2001.
7 B. Van Averbeke and D. Beljonne, Conformational Effects on Excitation Transport along Conjugated Polymer Chains, *J. Phys. Chem. A*, 2009, **113**, 2677–2682.
8 K. Becker, E. Da Como, J. Feldmann, F. Scheliga, E. T. Csanyi, S. Tretiak and J. M. Lupton, How chromophore shape determines the spectroscopy of phenylene-vinylenes: origin of spectral broadening in the absence of aggregation, *J. Phys. Chem. B*, 2008, **112**, 4859–4864.
9 S. Tretiak, A. Saxena, R. Martin and A. Bishop, Conformational dynamics of photoexcited conjugated molecules, *Phys. Rev. Lett.*, 2002, **89**, 97402–97406.
10 D. Tomalia and J. Fréchet, *Dendrimers and Other Dendritic Polymers*, John Wiley & Sons Ltd, West Sussex, England, 2001.
11 B. Balzani, M. Venturi and A. Credi, *Molecular Devices and Machines: A Journey into the Nanoworld*, Wiley-VCH Verlag GmbH & Co. KGaA, Weinheim, Germany, 2003.
12 A. Bosman, H. Janssen and E. Meijer, About Dendrimers: Structure, Physical Properties, and Applications, *Chem. Rev.*, 1999, **99**(7), 1665–1688.
13 A. Adronov and J. Fréchet, Light-harvesting dendrimers, *Chem. Commun.*, 2000, 1701–1710.
14 V. Balzani, P. Ceroni, M. Maestri and V. Vicinelli, Light-harvesting dendrimers, *Curr. Opin. Chem. Biol.*, 2003, **7**, 657–665.
15 A. Nantalaksakul, D. Reddy, C. Bardeen and S. Thayumanavan, Light Harvesting Dendrimers, *Photosynth. Res.*, 2006, **87**, 133–150.
16 T. Aida, D.-L. Jiang, E. Yashima and Y. Okamoto, A new approach to light-harvesting with dendritic antenna, *Thin Solid Films*, 1998, **331**, 254–258.

17 Y. Kim and S. Zimmerman, Applications of dendrimers in bio-organic chemistry, *Curr. Opin. Chem. Biol.*, 1998, **2**, 733–742.
18 D. Astruc and E. Boisselier, Dendrimers Designed for Functions: From Physical, Photophysical, and Supramolecular Properties to Applications in Sensing, Catalysis, Molecular Electronics, Photonics, and Nanomedicine, *Chem. Rev.*, 2010, 1857–1959.
19 S. Mukamel, Trees to trap photons, *Nature*, 1997, **388**, 425–427.
20 J. M. Fréchet, Functional polymers and dendrimers: reactivity, molecular architecture, and interfacial energy, *Science*, 1994, **263**, 1710–1715.
21 E. Atas, Z. H. Peng and V. D. Kleiman, Energy transfer in unsymmetrical phenylene ethynylene dendrimers, *J. Phys. Chem. B*, 2005, **109**, 13553–13560.
22 J. S. Melinger, Y. C. Pan, V. D. Kleiman, Z. H. Peng, B. L. Davis, D. McMorrow and M. Lu, Optical and photophysical properties of light-harvesting phenylacetylene monodendrons based on unsymmetrical branching, *J. Am. Chem. Soc.*, 2002, **124**, 12002–12012.
23 W. Ortiz, B. P. Krueger, V. D. Kleiman, J. L. Krause and A. E. Roitberg, Energy Transfer in the Nanostar: The Role of Coulombic Coupling and Dynamics, *J. Phys. Chem. A*, 2005, **109**, 11512–11519.
24 Y. Pan, M. Lu, Z. Peng and J. S. Melinger, Synthesis and optical properties of unsymmetrical conjugated dendrimers focally anchored with perylenes in different geometries, *J. Org. Chem.*, 2003, **68**, 6952–6958.
25 R. Kopelman, M. Shortreed, Z. Y. Shi, W. Tan, Z. Xu, J. S. Moore, A. Bar-Haim and J. Klafter, Spectroscopic Evidence for Excitonic Localization in Fractal Antenna Supermolecules, *Phys. Rev. Lett.*, 1997, **78**, 1239.
26 J. L. Palma, E. Atas, L. Hardison, T. B. Marder, J. C. Collings, A. Beeby, J. S. Melinger, J. L. Krause, V. D. Kleiman and A. E. Roitberg, Electronic Spectra of the Nanostar Dendrimer: Theory and Experiment, *J. Phys. Chem. C*, 2010, **114**, 20702–20712.
27 K. Gaab, A. Thompson, J. Xu, T. Martnez and C. Bardeen, Meta-Conjugation and Excited-State Coupling in Phenylacetylene Dendrimers, *J. Am. Chem. Soc.*, 2003, **125**, 9288–9289.
28 O. P. Varnavski, J. C. Ostrowski, L. Sukhomlinova, R. J. Twieg, G. C. Bazan and T. Goodson, Coherent Effects in Energy Transport in Model Dendritic Structures Investigated by Ultrafast Fluorescence Anisotropy Spectroscopy, *J. Am. Chem. Soc.*, 2002, **124**, 1736–1743.
29 A. L. Thompson, K. M. Gaab, J. J. Xu, C. J. Bardeen and T. J. Martinez, Variable electronic coupling in phenylacetylene dendrimers: the role of forster, dexter, and charge-transfer interactions, *J. Phys. Chem. A*, 2004, **108**, 671–682.
30 M. R. Shortreed, S. F. Swallen, Z. Y. Shi, W. Tan, Z. Xu, C. Devadoss, J. S. Moore and R. Kopelman, Directed Energy Transfer Funnels in Dendrimeric Antenna Supermolecules, *J. Phys. Chem. B*, 1997, **101**, 6318–6322.
31 Z. Xu, M. Kahr, K. L. Walker, C. L. Wilkins, J. S. Moore and J. S. M. Jj, Phenylacetylene Dendrimers by the Divergent, Convergent, and Double-Stage Convergent Methods Phenylacetylene Dendrimers by the Divergent, Convergent, and Double-Stage Convergent Methods, *J. Am. Chem. Soc.*, 1994, **116**, 4537–4550.
32 S. Swallen, Z. Shi, W. Tan, Z. Xu, J. Moore and R. Kopelman, Exciton localization hierarchy and directed energy transfer in conjugated linear aromatic chains and dendrimeric supermolecules, *J. Lumin.*, 1998, **76–77**, 193–196.
33 C. Devadoss, P. Bharathi and J. S. Moore, Energy Transfer in Dendritic Macromolecules: Molecular Size Effects and the Role of an Energy Gradient, *J. Am. Chem. Soc.*, 1996, **118**, 9635–9644.
34 A. Davydov, *Theory of Molecular Excitons*, Plenum, New York, 1971.
35 *Excitons*, ed. M. Rashba and E. I. Sturge, North Holland, Amsterdam, 1982.
36 V. Broude, E. Rashba and E. Sheka, *Spectroscopy of Molecular Excitons*, Springer, Berlin, 1985.
37 E. Y. Poliakov, V. Chernyak, S. Tretiak and S. Mukamel, Exciton-scaling and optical excitations of self-similar phenylacetylene dendrimers, *J. Chem. Phys.*, 1999, **110**, 8161–8175.
38 S. F. Swallen, R. Kopelman, J. S. Moore and C. Devadoss, Dendrimer photoantenna supermolecules: energetic funnels; exciton hopping and correlated excimer formation, *J. Mol. Struct.*, 1999, **486**, 585–597.
39 E. Ostroumov, R. Mulvaney, R. Cogdell and G. Scholes, Broadband 2D Electronic Spectroscopy Reveals a Carotenoid Dark State in Purple Bacteria, *Science*, 2013, **340**, 52–56.
40 A. Bakulin, C. Silva and E. Vella, Ultrafast Spectroscopy with Photocurrent Detection: Watching Excitonic Optoelectronic Systems at Work, *J. Phys. Chem. Lett.*, 2016, **7**, 250–258.
41 G. Soavi, F. Scotognella, G. Lanzani and G. Cerullo, Ultrafast Photophysics of Single-Walled Carbon Nanotubes, *Adv. Opt. Mater.*, 2016, **4**, 1670–1688.
42 J. Galindo, E. Atas, A. Altan, D. Kuroda, S. Fernandez-Alberti, S. Tretiak, A. Roitberg and V. Kleiman, Dynamics of Energy Transfer in a Conjugated Dendrimer Driven by Ultrafast Localization of Excitations, *J. Am. Chem. Soc.*, 2015, **137**, 11637–11644.
43 S. Bradforth, R. Jimenez, F. van Mourik, R. van Grondelle and G. Fleming, Excitation Transfer in the Core Light-Harvesting Complex (LH-1) of Rhodobacter sphaeroides: An Ultrafast Fluorescence Depolarization and Annihilation Study, *J. Phys. Chem.*, 1995, **99**, 16179–16191.
44 R. Camacho, S. Tubasum, J. Southall, R. Cogdell, G. Sforazzini, H. Anderson, T. Pullerits and I. Scheblykin, Fluorescence Polarization Measures Energy Funneling in Single Light-Harvesting Antennas – LH2 *vs.* Conjugated Polymers, *Sci. Rep.*, 2015, **5**, 15080.
45 C.-K. Yong, P. Parkinson, D. Kondratuk, W.-H. Chen, A. Stannard, A. Summerfield, J. Sprafke, M. O'Sullivan, P. Beton and H. Anderson, *et al.*, Ultrafast Delocalization of

Excitation in Synthetic Light-Harvesting Nanorings, *Chem. Sci.*, 2015, **6**, 181–189.

46 J. Johnson, R. Chen, X. Chen, A. Moskun, X. Zhang, S. Hogen-Esch and T. E. Bradforth, Investigation of Macrocyclic Polymers as Artificial Light Harvesters: Subpicosecond Energy Transfer in Poly(9,9-Dimethyl-2-Vinylfluorene), *J. Phys. Chem. B*, 2008, **112**, 16367–16381.

47 A. Aggarwal, A. Thiessen, A. Idelson, D. Kalle, D. Würsch, T. Stangl, F. Steiner, S.-S. Jester, J. Vogelsang, S. Höger and E. Al, Fluctuating Exciton Localization in Giant π-Conjugated Spoked-Wheel Macrocycles, *Nat. Chem.*, 2013, **5**, 964–970.

48 O. Varnavski, I. Samuel, L.-O. Palsson, R. Beavington, P. Burn and T. Goodson, Investigations of Excitation Energy Transfer and Intramolecular Interactions in a Nitrogen Corded Distrylbenzene Dendrimer System, *J. Chem. Phys.*, 2002, **116**, 8893.

49 S. Schmid, K. Yim, M. Chang, Z. Zheng, W. Huck, R. Friend, J. Kim and L. Herz, Polarization Anisotropy Dynamics for Thin Films of a Conjugated Polymer Aligned by Nanoimprinting, *Phys. Rev. B: Condens. Matter Mater. Phys.*, 2008, **77**, 115338.

50 T. Dykstra, E. Hennebicq, D. Beljonne, J. Gierschner, G. Claudio, E. Bittner, J. Knoester and G. Scholes, Conformational Disorder and Ultrafast Exciton Relaxation in PPV-family Conjugated Polymers, *J. Phys. Chem. B*, 2009, **113**, 656–667.

51 I. Yamazaki, S. Akimoto, T. Yamazaki, S.-I. Sato and Y. Sakata, Oscillatory Exciton Transfer in Dithiaanthracenophane: Quantum Beat a Coherent Photochemical Process in Solution, *J. Phys. Chem. A*, 2002, **106**, 2122–2128.

52 F. Zhu, C. Galli and R. Hochstrasser, The Real-Time Intramolecular Electronic Excitation Transfer Dynamics of 9′,9-Bifluorene and 2′,2-Binaphtyl in Solution, *J. Chem. Phys.*, 1993, **98**, 1042–1057.

53 S. Tretiak, V. Chernyak and S. Mukamel, Localized Electronic Excitations in Phenylacetylene Dendrimers, *J. Phys. Chem. B*, 1998, **102**, 3310–3315.

54 K. Harigaya, Optical excitations in diphenylacetylene based dendrimers studied by a coupled exciton model with off-diagonal disorder, *Int. J. Mod. Phys. B*, 1999, **13**, 2531–2544.

55 M. Takahata, M. Nakano, S. Yamada and K. Yamaguchi, One- and Two-Exciton Migration Dynamics of a Dendritic Molecular Aggregate, *Int. J. Quantum Chem.*, 2003, **95**, 472–478.

56 J. C. Kirkwood, C. Scheurer, V. Chernyak and S. Mukamel, Simulations of energy funneling and time- and frequency-gated fluorescence in dendrimers, *J. Chem. Phys.*, 2001, **114**, 2419–2429.

57 M. Takahata, M. Nakano, H. Fujita and K. Yamaguchi, Mechanism of exciton migration of dendritic molecular aggregate: a master equation approach including weak exciton–phonon coupling, *Chem. Phys. Lett.*, 2002, **363**, 422–428.

58 M. Takahata, M. Nakano and K. Yamaguchi, Exciton migration in dendritic aggregate systems using the quantum master equation approach involving weak exciton–phonon coupling, *J. Theor. Comput. Chem.*, 2003, **2**, 459–479.

59 M. Nakano, R. Kishi, M. Takahata, T. Nitta and K. Yamaguchi, Exciton dynamics in nanostar dendritic systems using a quantum master equation approach: core monomer effects and possibility of energy transport control, *J. Lumin.*, 2005, **111**, 359–366.

60 T. Tada, D. Nozaki, M. Kondo and K. Yoshizawa, Molecular Orbital Interactions in the Nanostar Dendrimer, *J. Phys. Chem. B*, 2003, **107**, 14204–14210.

61 S. Fernandez-Alberti, V. D. Kleiman, S. Tretiak and A. E. Roitberg, Nonadiabatic molecular dynamics simulations of the energy transfer between building blocks in a phenylene ethynylene dendrimer, *J. Phys. Chem. A*, 2009, **113**, 7535–7542.

62 S. Fernandez-Aberti, V. D. Kleiman, S. Tretiak and A. E. Roitberg, Unidirectional energy transfer in conjugated molecules: the crucial role of high frequency C (triple) C bonds, *J. Phys. Chem. Lett.*, 2010, **1**, 2699–2704.

63 S. Fernandez-Alberti, A. E. Roitberg, V. D. Kleiman, T. Nelson and S. Tretiak, Shishiodoshi unidirectional energy transfer mechanism in phenylene ethynylene dendrimers, *J. Chem. Phys.*, 2012, **137**, 22A526.

64 D. Ondarse-Alvarez, S. Kömürlü, A. Roitberg, G. Pierdominici-Sottile, S. Tretiak, S. Fernandez-Alberti and V. Kleiman, Ultrafast electronic energy relaxation in a conjugated dendrimer leading to inter-branch energy redistribution, *Phys. Chem. Chem. Phys.*, 2016, **18**, 25080–25089.

65 J. Liu and W. Thiel, An efficient implementation of semi-empirical quantum-chemical orthogonalization-corrected methods for excited-state dynamics, *J. Chem. Phys.*, 2018, **154103**, 154103.

66 J. Huang, L. Du, J. Wang and Z. Lan, Photoinduced excited-state energy-transfer dynamics of a nitrogen-cored symmetric dendrimer: from the perspective of the Jahn-Teller effect, *J. Phys. Chem. C*, 2015, **119**, 7578–7589.

67 V. Chernyak, E. Y. Poliakov, S. Tretiak and S. Mukamel, Two-exciton states and spectroscopy of phenylacetylene dendrimers, *J. Chem. Phys.*, 1999, **111**, 4158–4168.

68 D. Rana and G. Gangopadhyay, Studies on energy transfer in dendrimer supermolecule using classical random walk model and Eyring model, *J. Chem. Phys.*, 2003, **118**, 434–443.

69 S. Raychaudhuri, Y. Shapir and S. Mukamel, Disorder and funneling effects on exciton migration in treelike dendrimers, *Phys. Rev. E: Stat., Nonlinear, Soft Matter Phys.*, 2002, **65**, 1–12.

70 S. Raychaudhuri, Y. Shapir, V. Chernyak and S. Mukamel, Excitonic funneling in extended dendrimers with nonlinear and random potentials, *Phys. Rev. Lett.*, 2000, **85**, 282–285.

71 M. A. Martín-Delgado, J. Rodriguez-Laguna and G. Sierra, Density-matrix renormalization-group study of excitons in dendrimers, *Phys. Rev. B: Condens. Matter Mater. Phys.*, 2002, **65**, 1–11.

72 A. Bar-Haim, J. Klafter and R. Kopelman, Dendrimers as controlled artificial energy antennae, *J. Am. Chem. Soc.*, 1997, **119**, 6197–6198.
73 A. Bar-haim and J. Klafter, Geometric versus Energetic Competition in Light Harvesting by Dendrimers, *J. Lumin.*, 1998, **5647**, 197–200.
74 T. Nelson, S. Fernandez-Alberti, A. E. Roitberg and S. Tretiak, Nonadiabatic Excited State Molecular Dynamics: Modeling Photophysics in Organic Conjugated Materials, *Acc. Chem. Res.*, 2014, **47**, 1155–1164.
75 A. Sifain, J. Bjorgaard, T. Nelson, B. Nebgen, A. White, B. Gifford, D. Gao, O. Prezhdo, S. Fernandez-Alberti, A. Roitberg and S. Tretiak, Photoexcited Nonadiabatic Dynamics of Solvated Push–Pull π-Conjugated Oligomers with the NEXMD Software, *J. Chem. Theory Comput.*, 2018, **14**, 3955–3966.
76 T. Nelson, S. Fernandez-alberti, V. Chernyak, A. E. Roitberg and S. Tretiak, Nonadiabatic Excited-State Molecular Dynamics Modeling of Photoinduced Dynamics in Conjugated Molecules, *J. Phys. Chem. B*, 2011, **115**, 5402–5414.
77 J. C. Tully, Molecular dynamics with electronic transitions, *J. Chem. Phys.*, 1990, **93**, 1061–1071.
78 S. Hammes-schiffer and J. C. Tully, Proton transfer in solution: molecular dynamics with quantum transitions, *J. Chem. Phys.*, 1994, **101**, 4657–4667.
79 S. Tretiak and S. Mukamel, Density matrix analysis and simulation of electronic excitations in conjugated and aggregated molecules, *Chem. Rev.*, 2002, **102**, 3171–3212.
80 V. Chernyak, M. F. Schulz, S. Mukamel, S. Tretiak and E. V. Tsiper, Krylov-space algorithms for time-dependent Hartree–Fock and density functional computations, *J. Chem. Phys.*, 2000, **113**, 36.
81 S. Tretiak, C. M. Isborn, A. M. N. Niklasson and M. Challacombe, Representation independent algorithms for molecular response calculations in time-dependent self-consistent field theories, *J. Chem. Phys.*, 2009, **130**, 054111.
82 F. Furche and R. Ahlrichs, Adiabatic time-dependent density functional methods for excited state properties, *J. Chem. Phys.*, 2002, **117**, 7433–7448.
83 S. Tretiak and V. Chernyak, Resonant nonlinear polarizabilities in the time-dependent density functional theory, *J. Chem. Phys.*, 2003, **119**, 8809–8823.
84 M. Tommasini, V. Chernyak and S. Mukamel, Electronic density-matrix algorithm for nonadiabatic couplings in molecular dynamics simulations, *Int. J. Quantum Chem.*, 2001, **85**, 225–238.
85 V. Chernyak and S. Mukamel, Density-matrix representation of nonadiabatic couplings in time-dependent density functional (TDDFT) theories, *J. Chem. Phys.*, 2000, **8**, 3572–3579.
86 R. Send and F. Furche, First-order nonadiabatic couplings from time-dependent hybrid density functional response theory: consistent formalism, implementation, and performance, *J. Chem. Phys.*, 2010, **132**, 044107.
87 S. Mukamel, S. Tretiak, T. Wagersreiter and V. Chernyak, Electronic coherence and collective optical excitations of conjugated molecules, *Science*, 1997, **277**, 781–787.
88 S. Tretiak, V. Chernyak and S. Mukamel, Recursive density-matrix-spectral-moment algorithm for molecular nonlinear polarizabilities, *J. Chem. Phys.*, 1996, **105**, 8914–8928.
89 S. Tretiak, W. M. Zhang, V. Chernyak and S. Mukamel, Excitonic couplings and electronic coherence in bridged naphthalene dimers, *Proc. Natl. Acad. Sci. U. S. A.*, 1999, **96**, 13003–13008.
90 M. J. S. Dewar, E. G. Zoebisch, E. F. Healy and J. J. P. Stewart, The development and use of quantum-mechanical molecular-models.76.AM1 – a new general purpose quantum-mechanical molecular-model, *J. Am. Chem. Soc.*, 1985, **107**, 3902–3909.
91 T. Nelson, S. Fernandez-Alberti, V. Chernyak, A. E. Roitberg and S. Tretiak, Nonadiabatic excited-state molecular dynamics: numerical tests of convergence and parameters, *J. Chem. Phys.*, 2012, **136**, 054108.
92 S. Tretiak, V. Chernyak and S. Mukamel, Two-dimensional real-space analysis of optical excitations in acceptor-substituted carotenoids, *J. Am. Chem. Soc.*, 1997, **119**, 11408–11419.
93 S. Tretiak, V. Chernyak and S. Mukamel, Collective electronic oscillators for nonlinear optical response of conjugated molecules, *Chem. Phys. Lett.*, 1996, **259**, 55–61.
94 C. Wu, S. V. Malinin, S. Tretiak and V. Y. Chernyak, Exciton scattering and localization in branched dendrimeric structures, *Nat. Phys.*, 2006, **2**, 631–635.
95 R. J. Bell, P. Dean and D. C. Hibbins-Butler, Localization of normal modes in vitreous silica, germania and beryllium fluoride, *J. Phys. C: Solid State Phys.*, 1970, **3**, 2111–2118.
96 S. N. Taraskin and S. R. Elliott, Anharmonicity and localization of atomic vibrations in vitreous silica, *Phys. Rev. B: Condens. Matter Mater. Phys.*, 1999, **59**, 8572–8585.
97 N. Oldani, S. K. Doorn, S. Tretiak and S. Fernandez-Alberti, Photoinduced dynamics in cycloparaphenylenes: planarization, electron–phonon coupling, localization and intraring migration of the electronic excitation, *Phys. Chem. Chem. Phys.*, 2017, **19**, 30914–30924.
98 L. Alfonso Hernandez, T. Nelson, M. F. Gelin, J. M. Lupton, S. Tretiak and S. Fernandez-Alberti, Interference of Interchromophoric Energy-Transfer Pathways in π-Conjugated Macrocycles, *J. Phys. Chem. Lett.*, 2016, **7**, 4936–4944.
99 M. A. Soler, A. Bastida, M. H. Farag, J. Zúñiga and A. Requena, A method for analyzing the vibrational energy flow in biomolecules in solution, *J. Chem. Phys.*, 2011, **135**, 204106.
100 J. Wang, R. Wolf, J. Caldwell, P. Kollman and D. Case, Development and testing of a general amber force field, *J. Comput. Chem.*, 2004, **25**, 1157–1174.
101 G. Mukherjee, N. Patra, P. Barua and B. Jayaram, A fast empirical GAFF compatible partial atomic charge assignment scheme for modeling interactions of small molecules with biomolecular targets, *J. Comput. Chem.*, 2011, **32**, 893–907.
102 P. Cieplak, W. Cornell, C. Bayly and P. Kollman, Application of the multimolecule and multiconformational RESP methodology to biopolymers – charge derivation for DNA, RNA, and proteins, *J. Comput. Chem.*, 1995, **16**, 1357–1377.

103 C. Bayly, P. Cieplak, W. Cornell and P. Kollman, A well-behaved electrostatic potential based method using charge restraints for deriving atomic charges – the RESP model, *J. Phys. Chem.*, 1993, **97**, 10269–10280.

104 S. Fernandez-Alberti, A. E. Roitberg, T. Nelson and S. Tretiak, Identification of unavoided crossings in non-adiabatic photoexcited dynamics involving multiple electronic states in polyatomic conjugated molecules, *J. Chem. Phys.*, 2012, **137**, 014512.

105 T. Nelson, S. Fernandez-alberti, A. E. Roitberg and S. Tretiak, Nonadiabatic Excited-State Molecular Dynamics: Treatment of Electronic Decoherence, *J. Chem. Phys.*, 2013, **138**, 224111.

106 T. Nelson, S. Fernandez-Alberti, A. E. Roitberg and S. Tretiak, Nonadiabatic excited-state molecular dynamics: modeling photophysics in organic conjugated materials, *Acc. Chem. Res.*, 2014, **47**, 1155–1164.

107 F. Feng, S. H. Lee, S. W. Cho, S. Kömürlü, T. D. McCarley, A. Roitberg, V. D. Kleiman and K. S. Schanze, Conjugated polyelectrolyte dendrimers: aggregation, photophysics, and amplified quenching, *Langmuir*, 2012, **28**, 16679–16691.

108 K. Nishioka and M. Suzuki, Dynamics of unidirectional exciton migration to the molecular periphery in a photoexcited compact dendrimer, *J. Chem. Phys.*, 2005, **122**, 024708.

109 D.-L. Jiang and T. Aida, Morphology-Dependent Photochemical Events in Aryl Ether Dendrimer Porphyrins: Cooperation of Dendron Subunits for Singlet Energy Transduction, *J. Am. Chem. Soc.*, 1998, **120**, 10895–11091.

110 M. A. Soler, A. E. Roitberg, T. Nelson, S. Tretiak and S. Fernandez-Alberti, Analysis of state-specific vibrations coupled to the unidirectional energy transfer in conjugated dendrimers, *J. Phys. Chem. A*, 2012, **116**, 9802–9810.

111 D. Ondarse-Alvarez, N. Oldani, S. Tretiak and S. Fernandez-Alberti, Computational study of photoexcited dynamics in bichromophoric cross-shaped oligofluorene, *J. Phys. Chem. A*, 2014, **118**, 10742–10753.

112 J. Clark, T. Nelson, S. Tretiak, G. Cirmi and G. Lanzani, Femtosecond Torsional Relaxation, *Nat. Phys.*, 2012, **8**, 225–231.

113 S. Karabunarliev, M. Baumgarten, E. Bittner and K. Mullen, Rigorous Franck Condon Absorption and Emission Spectra of Conjugated Oligomers from Quantum Chemistry, *J. Chem. Phys.*, 2000, **113**, 11372–11381.

114 M. Kasha, Characterization of Electronic Transitions in Complex Molecules, *Discuss. Faraday Soc.*, 1950, **9**, 14–19.